# Effects of climate change on methane emissions from seafloor sediments in the Arctic Ocean: A review

Rachael H. James[1], Philippe Bousquet[2], Ingeborg Bussmann[3], Matthias Haeckel[4], Rolf Kipfer[5,6,7], Ira Leifer[8], Helge Niemann[9,10], Ilia Ostrovsky[11], Jacek Piskozub[12], Gregor Rehder[13], Tina Treude[14], Lisa Vielstädte[4], and Jens Greinert[4,10,15]

[1]Ocean and Earth Science, National Oceanography Centre Southampton, University of Southampton Waterfront Campus, European Way, Southampton SO14 3ZH, UK

[2]Laboratoire des Sciences du Climat et de l'Environnement, CEA Saclay, Orme de Merisiers, 91191 Gif sur Yvette, France

[3]Alfred Wegener Institut Helmholtz-Zentrum für Polar- und Meeresforschung, Kurpromenade 201, 27498 Helgoland, Germany

[4]GEOMAR Helmholtz Centre For Ocean Research Kiel, Wischhofstrasse 1-3, 24148 Kiel, Germany

[5]Eawag, Swiss Federal Institute of Aquatic Science and Technology, CH-8600 Dübendorf, Switzerland

[6]Institute of Biogeochemistry and Pollutant Dynamics, Swiss Federal Institute of Technology (ETH), CH-8092 Zurich, Switzerland

[7]Institute of Geochemistry and Petrology, Swiss Federal Institute of Technology (ETH), CH-8092 Zurich, Switzerland

[8]Bubbleology Research International, Solvang, CA 93463, USA

[9]Department of Environmental Sciences, University of Basel, 4056 Basel, Switzerland

[10]CAGE – Centre for Arctic Gas Hydrate, Environment and Climate, Department of Geology, UiT The Arctic University of Norway, 9037 Tromsø, Norway

[11]Israel Oceanographic & Limnological Research, Yigal Allon Kinneret Limnological Laboratory, Migdal 14950, Israel

[12]Institute of Oceanology, Polish Academy of Sciences, Sopot 81-712, Poland

[13]Leibniz Institute for Baltic Sea Research Warnemünde, Seestr. 15, 18119 Rostock, Germany

[14]Department of Earth, Planetary & Space Sciences and Atmospheric & Oceanic Sciences, University of California, Los Angeles, Los Angeles, CA 90095, USA

[15]Christian Albrechts University Kiel, Kiel, Germany

Corresponding author: Rachael H. James (R.H.James@soton.ac.uk)

Running head: Methane emissions from Arctic sediments

Key words: methane, Arctic Ocean, sediments, oxidation, gas hydrate, climate change

**Abstract**

Large quantities of methane are stored in hydrates and permafrost within shallow marine sediments in the Arctic Ocean. These reservoirs are highly sensitive to climate warming, but the fate of methane released from sediments is uncertain. Here we review the principal physical and biogeochemical processes that regulate methane fluxes across the seabed, the fate of this methane in the water column, and potential for its release to the atmosphere. We find that, at present, fluxes of dissolved methane are significantly moderated by anaerobic and aerobic oxidation of methane. If methane fluxes increase then a greater proportion of methane will be transported by advection or in the gas phase, which reduces the efficiency of the methanotrophic sink. Higher freshwater discharge to Arctic shelf seas may increase stratification and inhibit transfer of methane gas to surface waters, although there is some evidence that increased stratification may lead to warming of sub-pycnocline waters, increasing the potential for hydrate dissociation. Loss of sea-ice is likely to increase wind speeds and sea-air exchange of methane will consequently increase. Studies of the distribution and cycling of methane beneath and within sea ice are limited, but it seems likely that the sea-air methane flux is higher during melting in seasonally ice-covered regions. Our review reveals that increased observations around especially the anaerobic and aerobic oxidation of methane, bubble transport, and the effects of ice cover, are required to fully understand the linkages and feedback pathways between climate warming and release of methane from marine sediments.

# Effects of climate change on methane emissions from seafloor sediments in the Arctic Ocean: A review

## Introduction

Arctic and sub-Arctic marine sediments are thought to host vast reservoirs of methane stored in methane hydrate (~100-9000 Gt C: Kvenvolden, 1988; Biastoch et al., 2011; Hunter et al., 2013; Kretschmer et al., 2015) and trapped beneath submerged permafrost either as hydrate, or as free gas (~2-1400 Gt C: McGuire et al., 2009; Shakhova et al., 2010) (Table 1). These carbon pools can be highly sensitive to increases in temperature, and they provide the basis for release of methane to the atmosphere where this greenhouse gas contributes to further global warming. As high latitudes of the northern hemisphere are expected to experience a larger temperature increase than other regions due to climate change (IPCC, 2013), there is a need to better understand the linkages between environmental variables and the processes that regulate methane emissions from Arctic marine sediments into the atmosphere (e.g. Biastoch et al., 2011; Ferré et al., 2012; Steinle et al., 2015).

### *Environmental change in the Arctic Ocean*

The Arctic Ocean is an intercontinental sea surrounded by the land masses of Alaska/USA, Canada, Greenland, Norway, Iceland and Siberia/Russia (Fig. 1). It represents about 1% of the global ocean volume but receives about 10% of global runoff (Lammers et al., 2001). It has a central deep basin and is characterized by extensive shallow shelf areas including the Barents Sea, Kara Sea, Laptev Sea, East Siberian Sea, Chukchi Sea and Beaufort Sea. Monitoring of Arctic Ocean waters has revealed that deeper waters of Atlantic origin have expanded in volume since 1993 (Carmack et al., 1995), although circulation models indicate that this phenomenon could have started as early as 1979 (Maslowski et al., 2000). These deep Atlantic waters are carried into the Arctic Ocean via the West Spitsbergen

Current, continuing into the European and Makarov basins where they contribute to a temperature increase which may be up to 1˚C above the pre-1999 mean (Walczowski and Piechura, 2006), and shoaling of Atlantic water by 75-90 m (Polyakov et al., 2010). Over the same period, the temperature of Pacific waters flowing into the Arctic Ocean through the Bering Strait has increased by ~0.5˚C (Woodgate et al., 2006), although bottom water temperatures along the Russian slope remain almost unchanged (Biastoch et al., 2011).

Parts of the Arctic Ocean off Canada and Greenland are ice-covered throughout the year, but the rest is ice free in the summer months. Sea-ice coverage has decreased in recent decades, especially in the summer, becoming both younger and thinner (Maslanik et al., 2007). Sea-ice extent reached a record low (since satellite measurements began) in September 2012 (http://nsidc.org/; Fig. 2), such that ~45% of the Eurasian Basin north of 78 ˚N was ice-free.

Both a simple extrapolation and numerical modelling suggest that the Arctic may be seasonally ice-free by 2050, or possibly earlier (Stroeve et al., 2008; Wang and Overland, 2009), although this is far from certain (Serreze, 2011). A seasonally ice-free ocean would influence Arctic ecology and climate, enhancing available solar irradiance, increasing mixing, and radically reducing the albedo of the Arctic Ocean during the boreal summer. Sea-ice decline seems to be related at least in part to increasing greenhouse gas concentrations as this is the only known climate forcing that has strengthened in recent decades (IPCC, 2013), although black soot may also play a role (Jacobsen, 2004). Further decline in sea-ice coverage can be reasonably expected as long as Arctic warming continues (Stroeve et al. 2011).

***Methane in Arctic marine sediments***

Methane is produced in marine sediments either by cracking of complex organic molecules at high temperatures and great depths, or by microbial transformation of organic or inorganic carbon at shallower depths (Reeburgh, 2007; Rother, 2010). At relatively low temperature (<10 ˚C) and moderate pressure (> 3-5 MPa, which corresponds to combined water and sediment depths of 300 to 500 m) conditions found on the Arctic continental slope and beyond, methane and water combine to form methane hydrate, an ice-like substance consisting of a methane molecule encaged by water molecules forming a solid (Sloan and Koh, 2007; Fig. 3). Methane occurs as free gas below the depth of the hydrate stability zone, and may be transferred directly into the overlying water column through faults and fractures in the sediments (e.g. Berndt, 2005; Sarkar et al., 2012; Smith et al., 2014).

In 2008, more than 250 plumes of methane bubbles were discovered issuing from the seafloor offshore western Svalbard, close to the depth at which the hydrate stability zone outcrops at the seafloor (~400 m; Westbrook et al., 2009). The methane emissions have been attributed, at least in part, to hydrate dissociation as a result of seasonal fluctuations in bottom water temperatures (Berndt et al., 2014), and warming of bottom waters in this area over the last ~30 years (Westbrook et al., 2009; Thatcher et al., 2013). In this connection, observations of methane-rich gas bubbles venting from the seafloor focused on pingo-like features on the Beaufort Sea shelf have also been attributed to gas hydrate decomposition driven by inundation of relatively warm water (Paull et al., 2007). Models of hydrate behaviour based on predictions of ocean warming offshore western Svalbard indicate that the seafloor methane flux from the continental slope and shelf region is likely to increase in future years (Marín-Moreno et al., 2013; Kretschmer et al., 2015). However, at the current time, direct methane emissions from the ocean offshore western Svalbard account for <10% of the atmospheric input to this region (Fisher et al., 2011; see also Gentz et al., 2014).

Extensive shallow-water areas of the Arctic continental shelf are underlain by permafrost (Rachold et al., 2007), which formed under terrestrial conditions and was subsequently submerged by post-glacial rise in sea level. Methane can be trapped within this permafrost, as well as below its base. In the Beaufort Sea, seismic data indicate that submerged permafrost is confined to relatively shallow water depths (< 20 m), within 30 km of the shoreline (Brothers et al., 2012). While methane concentrations in seafloor sediments in the Beaufort Sea are relatively high (Coffin et al., 2013; Treude et al., 2014), there is no evidence for bubble seepage from the seafloor, and there are no systematic changes in methane concentrations close to the seafloor between nearshore sediments underlain by permafrost, and those lacking such permafrost (Pohlman et al., 2012). By contrast, partial thawing of permafrost on the shallow (average depth ~45 m) East Siberian Arctic Shelf is considered to be responsible for very high dissolved methane concentrations in the water column (>500 nM) and elevated methane concentrations in the atmosphere, by 5 to 10% up to 1800 m in height above the sea surface (Shakhova et al., 2014). Other authors have shown that, in the Laptev Sea, methane released from thawing permafrost is efficiently oxidised in the overlying unfrozen sediments, such that methane concentrations in the water column were close to normal background levels (Overduin et al., 2015).

***Scope of this review***

The work outlined above provides evidence for ongoing and possibly increasing release of methane stored within seafloor sediments in the Arctic Ocean, which may be linked to changing environmental conditions. The processes that regulate methane fluxes across the seabed, the fate of this methane in the water column, and its flux to the atmosphere, are however poorly understood. Moreover, these processes are not currently considered at all in global climate and Earth system models. With this in mind, this review sets out to identify the

principal physical and biogeochemical processes that regulate methane distributions in Arctic seafloor sediments, its fate if transferred into the water column, and the controls on subsequent release of methane to the atmosphere. The possible effects of future climate warming on all of these processes are also discussed.

## Processes affecting methane distributions in Arctic marine sediments

### *Transport processes through the sediment*

In the porous sediment matrix, methane dissolved in pore waters is transported by diffusion and advection, and as gas by buoyancy in form of individual bubbles or a continuous gas phase. Diffusive transport is driven by the methane concentration gradient in the aqueous phase according to Fick's first law of diffusion (Fick, 1855), following a tortuous path around the sediment grains, which is usually expressed as a function of sediment porosity (e.g. Bear, 1972; Boudreau, 1996; Tomonaga et al., 2015). Pore water advection and gas migration are driven by pressure gradients and are typically described by Darcy's equation (Darcy, 1856; Bear, 1972). Hence, they are affected by sediment permeability and fluid/gas viscosity.

In passive marine margin settings (i.e. margins that are unaffected by tectonic processes), diffusion and burial of pore water (due to sediment accumulation) are the governing transport mechanisms. In these settings, methane is usually completely consumed within the sediment by anaerobic oxidation of methane (AOM) (Reeburgh, 2007; Knittel and Boetius, 2009; see below).

In active marine margin environments, external (tectonic) pressure forces, together with high sedimentation rates and compaction, induce upward fluid flow that can exceed the (downward) burial velocity resulting in fluid expulsion from the sediment into the overlying water column at velocities of several millimetres to 1-2 meters per year. However, high fluid

179 velocities are locally confined to focused fluid flow pathways which are expressed as
180 pockmarks, mud volcanoes, or carbonate pavements. In the Arctic Ocean, methane produced
181 at depth in marine sediments has been observed venting from pockmarks offshore Western
182 Svalbard (Fig. 4), as well as on the Vestnesa Ridge (e.g. Smith et al., 2014), from the Haakon
183 Mosby mud volcano in the Barents Sea (e.g. Felden et al., 2010; Pape et al., 2011), and in
184 Disko Bay, east Greenland (Nielsen et al., 2014).

185 If sedimentary methane fluxes are high, for example at the landward limit of the gas
186 hydrate stability zone (Fig. 3), or at sub-seafloor faults that intersect deeper gas-rich layers,
187 methane solubility in the local pore waters may be exceeded. In these circumstances, free gas
188 is formed which migrates through the sediments and is released into the overlying water
189 column as methane bubbles (Fig. 4). In contrast to diffusion and fluid flow, which are quite
190 well understood (e.g. de Beer et al., 2006), our knowledge about gas migration in the
191 subsurface in the marine environment is limited and accurate mechanistic models for gas
192 migration by ebullition are only slowly being developed (Boudreau et al., 2005).

193 The upper part of the sediment sequence on large parts of the Arctic shelf consists of
194 glacigenic sediments (glacial diamictons) that are extremely poorly sorted and have low
195 porosity (~30%), due to smaller grains filling pore spaces between larger grains, and very low
196 intergranular permeability (~ $10^{-17}$ $m^2$) (Hubbard and Maltman, 2000). This impedes vertical
197 migration of methane dissolved in fluid. In permafrost horizons, sediment permeability is
198 principally controlled by freezing of pore waters, which provides a perfect seal for upward
199 migrating fluids and gases. Subsequent thawing of this ice barrier as a result of warming will
200 open up pathways for fluid and gas seepage again. Gas hydrates also form a barrier to fluid
201 and gas seepage, but the seal is usually incomplete (Naudts et al., 2006). In the same context,
202 permafrost and gas hydrate thus provide increased geomechanical strength to the sediment
203 matrix.

If hydrate dissociates, for example as a result of warming, the gas produced will increase pressure in sediment of low permeability, creating cracks or even causing the sediment matrix to collapse abruptly, leading to slumping and collapse structures (e.g. pockmarks; Fig. 4) (e.g. Vanneste et al., 2007). The presence of cracks increases the effective permeability of glacigenic sediments by around 4 orders of magnitude, to ~$10^{-13}$ $m^2$ (Thatcher et al., 2013), increasing the likelihood of gas flow at the seabed.

The colder water column in the Arctic Ocean allows methane to accumulate as hydrate in sediments in shallower water depths than is possible in most other parts of the world's oceans (Fig. 2), and it is this hydrate that climate warming will reach soonest and most strongly (e.g. Hunter et al., 2013). A number of recent modelling studies have assessed the potential for seafloor methane release in the Arctic Ocean as a result of hydrate dissociation based on observed and predicted warming scenarios (e.g. Reagan and Moridis, 2009; Biastoch et al., 2011; Reagan et al., 2011; Thatcher et al., 2013). Although the process of dissociation is endothermic (i.e. it requires heat), and the increase in pressure caused by released gas and the salinity decrease caused by released water both increase the stability of hydrate, most of the modelling studies agree that bottom water warming over the past 30 years (e.g. Walczowski and Piechura, 2006; Westbrook et al., 2009) is already likely to have resulted in increased methane fluxes across the seabed as a result of hydrate dissociation, and that these fluxes are expected to increase if warming were to accelerate in the future.

**The microbial methane filter in Arctic marine sediments**

After reduction by photochemical processes in the troposphere, microbial consumption is the largest sink of methane on our planet (Reeburgh, 2007; Hinrichs and Boetius, 2002). Pioneering work in the 1970's and 1980's (e.g. Martens and Berner, 1974; Zehnder and Brock, 1980) showed that a significant fraction of the methane that is produced

in seafloor sediments is retained in the anoxic part of the sediment column, apparently oxidised with sulphate as the terminal electron acceptor by a process known as 'anaerobic oxidation of methane' (AOM; see reviews by Reeburgh (2007) and Knittel and Boetius (2009) and references therein):

$$CH_4\,(aq) + SO_4^{2-}\,(aq) \rightarrow HCO_3^-\,(aq) + HS^-(aq) + H_2O \qquad \text{(Eq. 1)}$$

As a result, upward migrating methane and downward diffusing sulfate (originating from seawater) are consumed in a distinct sediment horizon, the so-called sulfate-methane transition zone (SMTZ) (Fig. 5). The yield of Gibbs free energy from AOM is however very small ($\Delta G^{o\prime} = -17$ kJ $mol^{-1}$), and AOM-mediating microorganisms have only been identified relatively recently. To date, three clades of anaerobic methane oxidisers (ANME-1, -2, -3) belonging to the euryarchaeota have been shown to mediate AOM. ANMEs often form aggregates with sulfate-reducing bacteria (SRB) of the genus *Desulfococcus*/*Desulfosarcina* (ANME-1, -2) or *Desulfobulbus* (ANME-3) (Hinrichs et al., 1999; Boetius et al., 2000; Niemann et al., 2006; see detailed review by Knittel and Boetius, 2009). However, the role of SRB in the AOM process is unclear.

In addition to sulfate-dependent AOM, recent studies have provided evidence for novel modes of AOM coupled to the reduction of oxidised metal species (Fe(III), Mn(IV)) (Beal et al., 2009; Sivan et al., 2011) and nitrite ($NO_2^-$) (Ettwig et al., 2010). However, the environmental significance of these pathways, particularly in marine environments, is yet to be determined.

In oxygen-replete surface sediments and the ocean water column, methane is oxidised aerobically with oxygen as the terminal electron acceptor (Fig. 5) (Hanson and Hanson, 1996; Murrel, 2010):

$$CH_4\,(aq) + 2O_2\,(aq) \rightarrow CO_2\,(aq) + 2H_2O \qquad \text{(Eq. 2)}$$

253 The yield of Gibbs free energy during aerobic methane oxidation (MOx) is relatively high
254 ($\Delta G°' = -820$ kJ $mol^{-1}$) compared to AOM. Nevertheless, MOx is of lesser importance in
255 shallow marine sediments as the penetration depth of oxygen into sediments is very limited.
256 Consequently, methane is typically consumed in the SMTZ via AOM, so significant
257 concentrations of oxygen and methane do not coexist in most marine sediments. However,
258 MOx becomes more important if methane bypasses the AOM filter and migrates into the oxic
259 water column (see below).

260 The ecology of AOM communities is not well understood, particularly for high-
261 latitude environments, so predicting the effects and feedback mechanisms of rising
262 temperatures in the Arctic and higher than present-day methane fluxes due to hydrate
263 dissociation and degradation of submerged permafrost remains, to a large extent, speculative.
264 Nevertheless, based on our knowledge of methane cycling at cold seeps, the following factors
265 are likely important in controlling methane fluxes across the seabed:

266 1. *Thermodynamic constraints*. AOM communities are typically found in a narrow sediment
267 horizon within the SMTZ (Knittel and Boetius, 2009). As the sulfate flux is dominated by
268 diffusion, an increase in the methane flux (which can be advective, see above) will
269 ultimately lead to an upward shift in the depth of the thermodynamic and kinetic optimum
270 for AOM (Niemann and Boetius, 2010).

271 2. *Microbial activity and growth*. To some degree, the AOM communities may
272 counterbalance an increase in methane flux by increasing their metabolic activity
273 (Nauhaus et al., 2002). The maximum velocity ($v_{max}$) of the AOM enzymatic machinery is
274 high (and the limit is not yet known: Nauhaus et al., 2002; Deusner et al., 2010), so it is
275 reasonable to assume that $v_{max}$ is probably not the limiting factor for efficient methane
276 consumption, even under future high methane flux regimes. However, large changes in the
277 methane flux will ultimately relocate the optimal depth for AOM (i.e. the SMTZ), as

described above. Thus, for efficient methane consumption, a new population of AOM communities must grow at the depth of the new SMTZ. The doubling time of ANME-2/DSS consortia is ~7 months (Nauhaus et al., 2007), so the genesis of an effective AOM microbial filter (typically consisting of $>10^{10}$ cells $cm^{-3}$: Lösekann et al., 2007; Knittel and Boetius, 2009) in sediments with only small ($<10^5$ cells $cm^{-3}$) AOM communities would be on the order of decades. Permeable sediments with fast exchange between sediment pore waters and the water column, i.e. fast supply of sulfate as well as removal of sulfide, could promote growth of AOM organisms (Wilfert et al., 2015), but they would also facilitate transfer of methane from sediments to the water column.

3. *Mode and magnitude of methane transport*. As discussed previously, methane is transported within sediments either in the dissolved phase (by diffusion or advection) or as free gas (ebullition of bubbles), which strongly controls the efficiency of the microbial methane filter. While the AOM communities may counterbalance increased transport of dissolved methane, they typically consume only a fraction of the advective methane flux (Treude et al., 2003; de Beer et al., 2006; Niemann et al., 2006). This is because free gas is inaccessible to microbes, which depend on a diffusive transmembrane gas transport. Thus while higher fluxes of methane will lead to higher concentrations of dissolved methane in pore waters, which likely increases rates of AOM (Treude et al., 2003), it increases the likelihood for transport of methane in the gas phase, which will bypass the sedimentary AOM filter. Changing methane flux regimes may also lead to shifts in the AOM community structure but, as yet, evidence for clear preferences of distinct AOM communities to specific habitats and flux regimes is limited (Knittel et al., 2005).
4. *Temperature*. In accordance with the van-'t-Hoff rule, increasing temperatures will stimulate AOM activity (e.g. Iversen and Blackburn, 1981), thus acting as a negative feedback to temperature induced increases in methane flux in a warming Arctic. However,

303 field (Iversen and Blackburn, 1981) as well as laboratory studies (Nauhaus et al., 2005)
304 indicate $Q_{10}$-values (i.e. the change of metabolic activity as a result of a 10 °C increase in
305 temperature) of 2 to 5. Thus, with respect to possible increases in bottom water
306 temperatures of 1-2 °C (Biastoch et al. 2011), it is questionable if the increase in metabolic
307 activity will be sufficient to counteract the higher methane flux (Shakhova et al., 2010).
308 Furthermore, the dissociation of gas hydrates consumes energy and therefore lowers the
309 temperature in the ambient sediments (Selim and Sloan, 1989), which could lead to the
310 opposite effect, i.e., a decrease in AOM activity. Changing temperatures may also lead to
311 compositional changes in the microbial community. Temperature preferences of AOM
312 communities are largely unknown but circumstantial evidence suggests that ANME-3 is
313 best adapted to the ice-cold temperatures of the Arctic region (Niemann et al., 2009).
314 5. *Elevated methane-derived biomass*. Higher methane fluxes will lead to an expansion of
315 present day cold seeps or, possibly, the formation of new systems. Thus, the amount of
316 methane-derived biomass and the development of hard substrates (methane derived
317 carbonates; Berndt et al., 2014) will increase as well. It therefore appears likely that
318 organisms consuming methane-derived biomass as well as those utilising hard substrates
319 will have an advantage in a future Arctic Ocean (Niemann et al., 2005; 2013).
320 Nevertheless, owing to an enormous influx of organic carbon from ice algae that is to be
321 expected as the ice caps melt (Boetius et al., 2013), the significance of increased biomass
322 due to higher sub-seafloor methane fluxes needs to be tested. Moreover, bioirrigation by
323 chemosynthetic organisms could strongly enhance methane consumption by increasing the
324 influx of electron acceptors from seawater into the organic-rich sediments (Cordes et al.,
325 2005; Niemann et al., 2006).
326
327 **Processes affecting methane distributions in the Arctic Ocean water column**

328 The three principal mechanisms that transfer methane from sediment to the overlying
329 water column are: (i) release of dissolved methane either by diffusion or fostered by
330 advective fluid flow, (ii) the release of gas bubbles, and (iii) rise of consolidated methane
331 hydrates, which may have a density lower than that of seawater, and thus become buoyant
332 when detached from the sediment matrix. Dissolved methane may be oxidised in the water
333 column under oxic conditions (Eq. 2).
334
335 ***Methane release from the seabed***
336 Where the methane flux is sufficiently high, methane escapes the seabed as bubbles
337 that rise singly or as a plume. The fate of a bubble released at the seafloor is critically
338 dependent on bubble size or radius, r. Small bubbles dissolve close to the seafloor, while
339 large bubbles can transport methane across hundreds of meters (Leifer and MacDonald,
340 2003). For example, for a singly rising bubble of radius r = 5mm, ~15% of its methane
341 reaches the atmosphere from 90 m water depth, while a bubble with r = 3 mm, released at the
342 same water depth, will dissolve within 8 m of the sea surface (Fig. 6; Leifer and Patro, 2002).
343 In the Arctic region, even gas bubbles with a relatively large radius (i.e. ~5 mm) will dissolve
344 completely within ~200 m of the seafloor (Fig. 6), which means that methane is unlikely to
345 be emitted directly into the atmosphere at water depths > ~200m. Methane bubbles released
346 at water depths within the gas hydrate stability zone will be encased by a hydrate skin, which
347 restricts bubble dissolution (Rehder et al., 2009). However, once the bubble rises above the
348 gas hydrate stability zone, the hydrate skin will rapidly dissociate and the rate of methane loss
349 from the bubble increases significantly (Fig. 6).
350 Bubble dissolution leads to approximately exponentially decreasing methane
351 concentrations with increasing distance above the seafloor (Leifer et al., 2006), and the
352 composition of the gas remaining in the rising bubble can considerably differ from the seabed

353 composition. Due to the higher partial pressure of gases dissolved in seawater ($N_2$, $O_2$, Ar)
354 and the different gas transfer rates across the bubble interface, in particular for nitrogen, a
355 bubble containing only methane at the seafloor can potentially reach the surface containing
356 mostly nitrogen and oxygen (Leifer and Patro, 2002; McGinnis et al., 2006; Schneider von
357 Deimling et al., 2011).

358 Methane from floating hydrates may be readily transported to the atmosphere (Brewer
359 et al., 2002), if the lower limit of the gas hydrate stability field is relatively close to the mixed
360 layer depth (e.g. the Arctic), as dissolution within the gas hydrate stability field is relatively
361 slow (Rehder et al., 2009) and decomposition occurs mainly after crossing the hydrate
362 stability boundary (Fig. 6). Decomposition leads to the formation of free gas, which
363 subsequently dissolves and may be subject to oxidation or sea-air exchange (see below). The
364 transport of methane by floating hydrates has been discussed in the framework of slope
365 failures (Paull et al., 2003), with prominent examples in the Arctic Ocean (e.g. Kvenvolden,
366 1999).

367 Dissolved methane that reaches the winter wave mixed layer by any of the processes
368 discussed above will be transported to the sea surface by wave mixing on time scales that are
369 usually shorter than the time scale for microbial degradation (see below), and will eventually
370 be partly expelled into the atmosphere. By contrast, bubble-mediated transport contributes
371 directly to atmospheric budgets. Winter storms deepen the pycnocline (Rudels et al., 1991),
372 and allow deeper water to be entrained into the surface mixed layer, as can local cross-
373 pycnocline transport mechanisms, such as upwelling (Rehder et al., 2002). However,
374 transport across the pycnocline is a rather slow process (e.g. Jakobs et al., 2014; Leifer et al.,
375 2015; Schneider von Deimling et al., 2015).

376 Most of the Arctic Ocean is permanently stratified with warmer, but more saline water
377 from the Atlantic and Pacific underlying a surface layer that is colder and fresher derived

from river runoff and ice melting (Yang et al., 2002). In the Arctic, freezing and melting have a major control on stratification, rather than thermal seasonal effects as elsewhere, leading to a pycnocline at 50 to 250 m (Rudels et al., 1991). The pycnocline presents a significant barrier for transport to the sea surface. Thus, methane below the pycnocline will mainly be transported laterally by currents, until storms deepen the mixed layer– potentially to the seabed in areas of shallow water. In the Barents Sea mixing can extend to deeper than 200 m (Rudels et al., 1991), and the Arctic is home to the largest shallow sea of the world's oceans, the East Siberian Arctic Sea (Semiletov et al., 2000), where frequent storms effectively vent the water column (Shakhova et al., 2014). The presence of polar lows, small intense short-lived cyclonic vortices that resemble tropical hurricanes (Emanuel, 1989), drives mixing deep through processes like Langmuir circulation (Smith, 1998). Thus, for dissolved methane above the winter mixed layer but below the pycnocline, lateral transport and sinking, such as that which occurs on outflow shelves (Carmack and Wassmann, 2006), could lead to submergence to depths where the primary fate is microbial oxidation. However, lateral transport also can lead to orographic upwelling or shoaling and more rapid transport to the atmosphere, particularly along inflow shelves (Carmack and Wassmann, 2006).

As Arctic sea-ice cover decreases, and sea surface temperature increases, evaporation will increase and precipitation is predicted to increase by >50% before the end of the 21$^{st}$ century (Bintanja and Selten, 2014). Between 1964 and 2000, river discharge to the Arctic Ocean increased by 5.6 km$^3$ yr$^{-1}$, mostly due to a large increase from the Eurasian rivers (McClelland et al., 2006). Modelling studies indicate that increased river runoff will strengthen stratification (e.g. Capotondi et al., 2012), producing a fresher and shallower surface mixed layer that may hinder delivery of methane from the seafloor to the sea surface. However, a recent study has suggested that increased stratification could increase the temperature of sub-pycnocline waters, at least on timescales of hundreds of years (Nummelin

et al., 2015). This could, in turn, increase the potential for hydrate dissociation. By contrast, decline in the summer extent of sea-ice (Fig. 2) enhances the strength and size of Arctic storms (e.g. Long and Perrie, 2012), and promotes vertical mixing between surface and deep waters (Pickart et al., 2013; Zhang et al., 2013). The relative strengths of these processes is likely to show significant regional variability; for example, areas affected by Atlantic inflow including the Greenland Sea and outer shelves of the Barents, Kara and Laptev seas, will experience greater vertical mixing (Popova et al., 2014). It is clear that future predictions of methane distributions in the water column are strongly reliant on reliable projections of freshwater fluxes and rates of sea-ice retreat, both of which are currently a major source of uncertainty in ocean circulation models.

***The microbial methane sink in the water column***

Organisms involved in MOx are found within several subdivisions of Proteobacteria and have been observed in a variety of terrestrial, limnic and marine environments (Hanson and Hanson, 1996; Treude et al., 2005; Niemann et al., 2006; Blumenberg et al., 2007; Lösekann et al., 2007; Elvert and Niemann, 2008; Steinle et al., 2015). Two biochemical pathways involved in MOx exist, the so-called RuMP and Serine pathways, which are utilised by Type I and Type II aerobic methanotrophs, respectively (Hanson and Hanson, 1996; Murrel, 2010 and references therein). A third MOx type, Type X, utilises both pathways.

The Arctic Ocean and shelf seas are generally well-oxidized so methane that escapes the sub-seafloor AOM filter and enters the water column is liable to be oxidized by MOx (Eq. 2). Studies conducted in very different marine settings report water column methane turnover times of the order of weeks to >1000 years (Fig. 7). Much shorter turnover times with rate constants of up to 15% $day^{-1}$ have been reported for hydrothermal plumes on the Juan de Fuca Ridge (Kadko et al., 1990; de Angelis et al., 1993). Methane turnover in methane-rich

428 water bodies, at cold vent sites, and above gas-bearing sediments, apparently takes place on
429 time scales of weeks to a few years (Valentine et al., 2010; Mau et al., 2013; Steinle et al.,
430 2015). Distinctly longer lifetimes have been reported for methane-poor seawater, from
431 several 10s to 50 years in cold newly-formed deep waters in the North Atlantic and the
432 Weddell Sea (Rehder et al., 1999; Heeschen et al., 2003), to several 100s of years in oceanic
433 deep waters with subnanomolar concentrations of methane (Scranton and Brewer, 1978). In
434 general, there is an inverse relationship between methane availability and turnover time (Fig.
435 7).

436 Nevertheless, the effectiveness of the microbial MOx filter is not well constrained,
437 particularly for Arctic environments where it may be dependent on variables in addition to
438 substrate availability (Reeburgh, 2007; Steinle et al., 2015), so we can only speculate as to
439 how the MOx filter will operate in a future Arctic Ocean. Ocean currents have recently been
440 identified as a globally important control for water column MOx activity above methane
441 point sources (Steinle et al., 2015). If currents are strong, the water mass residence time is
442 comparatively short which hampers the development of MOx communities. On the other
443 hand, seeding of MOx bacteria directly from the sediment into the water column through
444 rising methane bubbles could counteract this effect (Schmale et al., 2015). Benthic MOx
445 bacteria have been found in association with gas bubbles rising from sediments, but their
446 survival/growth rate and methane consumption efficiency in the water column is unclear.

447 Given that modelling work predicts that the aerobic methane oxidation rate is a key
448 control on emission of methane to the atmosphere in shallow Arctic shelf seas (Wåhlström
449 and Meier, 2014), further work on water column methane oxidation is consequently of
450 paramount importance for our understanding of methane release from the Arctic Ocean.
451 Furthermore, to the best of our knowledge, there have been no investigations on the effect of
452 ice cover on methane oxidation in marine environments. It is reasonable to assume that

methane from bubbles trapped beneath ice will slowly disperse, which may attract MOx communities (Rudd et al. 1976; 1978) and, in support of this, active methane oxidation has been reported beneath the Greenland ice sheet (Dieser et al., 2014). By contrast, changes in the the extent and / or duration of ice coverage of the Arctic Ocean mean that it is possible that methanotrophic bacteria will have less time to consume methane so the methane flux to the atmosphere will increase. Although there appears to be a direct relationship between sea-ice decline and increasing methane emissions in the Arctic, the contribution of oceanic methane sources is, as yet, unclear (Parmentier et al., 2013).

**Methane exchange across the sea-air interface**

Diffusive transport across the sea surface for a sparingly soluble gas like methane can be described as gas transfer across a resistive aqueous phase boundary layer driven by a concentration gradient (e.g. Liss, 1973). Waves and shear stress increase turbulence and reduce the thickness of the boundary layer, leading to higher exchange rates. With the onset of wave breaking, bubbles significantly enhance gas exchange (Carmack and Wassmann, 2006). For practical reasons, wind speed is usually the only non-gas specific variable used to quantify the gas transfer rate (e.g. Wanninkhof et al., 2009), although fetch dependency is well known (Liss and Merlivat, 1986) and important in polynyas and areas of mixed open water and ice. Large field experiments suggest gas exchange rates increase quadratically (Wanninkhof, 1992), cubically (Wanninkhof and McGillis, 1999), or between these two (Nightingale et al., 2000), as a function of wind speed. A recent review on advances and the state of the art of the parameterization of gas transfer velocities is given in Wanninkhof et al. (2009). Recent observations in the Arctic Ocean indicate that fast winds during storms considerably enhance methane emission at the sea surface (Shakhova et al., 2014), although

477 the integrated amount of methane released during these events and also all year long remain
478 heavily debated (Berchet et al., 2014).
479 Reductions in sea-ice coverage in the Arctic Ocean mean that larger waves are likely
480 and swells will be more common (Thomson and Rogers, 2014), as well as greater input of
481 water vapour into the atmosphere. Larger swells carry more energy and are more effective
482 both in breaking up sea-ice and vertically mixing surface waters. Both of these effects will
483 increase sea-air gas exchange in a future seasonally ice-free Arctic Ocean.
484 Most circulation models predict stronger winds and storm tracks migrating closer to
485 the pole as Arctic climate warms (IPCC, 2013), which would increase sea-air exchange.
486 However, some studies suggest that the number of polar lows (small short-lived intense
487 cyclonic vortices that resemble tropical hurricanes; Emanuel, 1989) may decline in a
488 warming world (Zahn and von Storch, 2010), and zonal circulation appears to have weakened
489 (reducing wind speeds) during recent winters (Francis et al., 2009). All of this points to the
490 conclusion that the effects of climate change on Arctic wind speeds (and consequently sea-air
491 gas flux) remain rather poorly constrained.
492

493 ***Effect of ice cover on sea-air gas exchange***

494 The formation of sea-ice, in particular in winter, gives potential for major restrictions
495 and alterations to the sea-air flux of methane. Even during the onset of ice formation, ice
496 crystals dampen wave formation at the surface and restrict free air-sea exchange (e.g. Loose
497 et al., 2014). Winter sea ice will almost completely suppress air-sea exchange, and a closed
498 sea ice cover will also trap bubbles reaching the surface. In this connection, a number of
499 studies report high methane concentrations under ice, both in the oceans and in lakes. On the
500 East Siberian Arctic shelf, dissolved methane concentrations beneath the sea ice are 5 to 10
501 times higher in winter, than they are in summer (Shakhova et al. 2010), and in the Canadian

Arctic, methane over-saturation has been found under multi-year sea-ice (Kitidis et al. 2010). It has been suggested that accumulation of methane under ice could enhance the annual sea-air flux due to release of this methane after melting in seasonally ice-covered regions (Lammers et al., 1995). In support of this, a more recent study has shown that sea-ice reduces methane emissions in the Arctic and continuous melting of sea-ice in the Arctic Ocean will drastically increase methane emissions to the atmosphere (He et al., 2013). Concentrations of atmopsheric methane have been shown to increase over open leads and regions with fractional sea-ice cover (Kort et al., 2012), providing further evidence that sea ice acts as a barrier to transfer of methane to the atmopshere. Finally, it has been demonstrated that methane release from the River Neva plume is delayed in winter in the seasonally ice-covered Gulf of Finland (Schneider et al., 2014).

**Summary and outlook**

Atmospheric methane concentrations have undergone significant changes in the past, and it is widely accepted that these have occurred in conjunction with shifts in global climate (e.g. Dickens, 2003; DeConto et al., 2012). Critically, it seems likely that Arctic methane emissions may have played a major role both in modern methane emissions (Dlugokencky et al., 2009) and in past global climatic change (Nisbet and Chappellaz, 2009).

Our synthesis of recent data indicates that the fate of methane in sub-seafloor Arctic Ocean reservoirs in a warming world is far from certain. Within the sediments, methane may be entirely consumed by AOM if methane fluxes are low. If methane fluxes increase, for example due to hydrate dissociation, AOM communities may increase their metabolic activity, but at the same time increased transport of methane as free gas will reduce the efficiency of the AOM filter. Gas hydrates and permafrost serve as a barrier to fluid and gas migration towards the seafloor but, if they melt, pressure will increase in low permeability

527 sediments creating cracks and fractures, which increase the likelihood of seabed gas flow.
528 Methane bubbles that enter the water column may be rapidly transported to the sea surface if
529 the bubbles are large and water depth is shallow. However, if the bubbles are small, or the
530 seabed is deep, and if the water column is strongly stratified, they will dissolve within a few
531 tens of meters above the seafloor and some fraction of the methane may be oxidised to $CO_2$
532 by aerobic methanotrophs. If seawater warms, the rate of bubble dissolution may decrease
533 but, on the other hand, increased river discharge to the Arctic Ocean is predicted to increase
534 stratification, inhibiting gas transport into the winter wave mixed surface layer. Stronger
535 winds will increase sea-air methane exchange, but the number of polar lows, which can strip
536 the water column of methane into the atmosphere, may decrease.
537
538 The effects of reduced sea-ice cover on methane emissions are especially poorly constrained.
539 Studies of the distribution and cycling of methane beneath sea-ice are almost absent from the
540 literature, and there have been no investigations on the effect of ice cover of methane
541 oxidation in marine environments. Improving our state of knowledge is vital as Arctic sea-ice
542 coverage continues to decrease.
543
544 Enhanced methane concentrations in the water column offshore western Svalbard, on the East
545 Siberian Arctic Shelf, and possibly in the Beaufort Sea, are likely related, at least in part, to
546 melting of gas hydrates and submerged permafrost. However, a critical question centres on
547 the timing of the response of these sub-seafloor methane reservoirs to Arctic environmental
548 change. Numerical modelling of the seafloor offshore western Svalbard predicts that the
549 delay between the onset of warming and emission of gas at the seafloor due to hydrate
550 dissociation may be less than 30 years (e.g. Thatcher et al., 2013), whereas dating of
551 authigenic carbonates suggests that methane seepage in this area has been ongoing for at least

552 3000 years (Berndt et al., 2014). Moreover, a recent study (Dmitrenko et al., 2011) suggests
553 that degradation of subsea permafrost is primarily related to warming initiated by permafrost
554 submergence about 8000 years ago, rather than recent Arctic warming. As abrupt release of
555 methane increases the likelihood of its release to the atmosphere, a better understanding of
556 the response of hydrate and submerged permafrost to increased temperatures, and especially
557 the identification of any non-linearity, is critical.
558
559 With the exception of $CO_2$, the biogeochemical transformations and physical processes that
560 affect the distributions of climatically active gases in the oceans are poorly represented in
561 Earth system models. Moreover, the role of sea bed processes currently is not considered at
562 all. This review reveals that there are numerous linkages and feedback pathways between
563 climate warming and release of methane from marine sediments, and there is clearly a
564 requirement to develop process-based models for methane. Increased observations, especially
565 for rates of anaerobic and aerobic oxidation of methane, bubble transport, and the effects of
566 ice cover, are needed to support these models. Closer collaboration between the observation
567 and modelling communities, so that the models have the ability to interface with
568 observations, that appropriate datasets are specified, and that they are then created in a
569 suitable format, is vital to this end.
570

571 **References**

572 Beal, E. J., C. H. House, and V. J. Orphan. 2009. Manganese- and iron-dependent marine
573 methane oxidation. Science 325: 184-187.

574 Bear, L. 1972. Dynamics of fluids in porous media. Dover Civil and Mechanical
575 Engineering Series. Dover Publishing.

576 Berchet, A., I. Pison, F. Chevallier, and others. 2014. Natural and anthropogenic methane
577 fluxes in Eurasia: a meso-scale quantification by generalized atmospheric inversion.
578 Biogeosciences Discuss. 11: 14587-14637, doi:10.5194/bgd-11-14587-2014

579 Berndt, C. 2005. Focused fluid flow in passive continental margins. Phil. Trans. Royal
580 Soc. A 363: 2855-2871.

581 Berndt, C., T. Feseker, T. Treude, and others. 2014. Temporal constraints on hydrate-
582 controlled methane seepage off Svalbard. Science 343: 284-287.

583 Biastoch, A., T. Treude, L. H. Rüpke, and others. 2011. Rising Arctic Ocean temperatures
584 cause gas hydrate destabilization and ocean acidification. Geophys. Res. Let. 38: L08602,
585 doi:08610.01029/02011GL047222

586 Bintanja, R., and F. M. Selten. 2014. Future increases in Arctic precipitation linked to
587 local evaporation and sea-ice retreat. Nature 509: 479-482.

588 Blumenberg, M., R. Seifert, and W. Michaelis. 2007. Aerobic methanotrophy in the oxic–
589 anoxic transition zone of the Black Sea water column. Org. Geochem. 38: 84-91.

590 Boetius, A., K. Ravenschlag, C. J. Schubert, and others. 2000. A marine microbial
591 consortium apparently mediating anaerobic oxidation of methane. Nature 407: 623-626.

592 Boetius, A., S. Albrecht, K. Bakker, and others. 2013. Export of algal biomass from the
593 melting Arctic sea ice. Science 339: 1430-1432.

594 Boudreau, B. P. 1996. The diffusive tortuosity of fine-grained unlithified sediments.
595 Geochim. Cosmochim. Acta 60: 3139-3142.

596 Boudreau, B. P., C. Algar, B. D. Johnson, and others. 2005. Bubble growth and rise in soft
597 sediments. Geology 33: 517-520.
598 Brewer, P. G., C. Paull, E. T. Peltzer, W. Ussler, G. Rehder, and G. Friederich. 2002.
599 Measurements of the fate of gas hydrates during transit through the ocean water column.
600 Geophys. Res. Lett. 29: 2081, doi:10.1029/2002GL014727
601 Brothers, L., P. Hart, and C. Ruppel. 2012. Minimum distribution of subsea ice-bearing
602 permafrost on the US Beaufort Sea continental shelf. Geophys. Res. Lett. 39: L15501,
603 doi:10.1029/2012GL052222
604 Capotondi, A., M. A. Alexander, N. A. Bond, E. N. Curchitser, and J. D. Scott. 2012.
605 Enhanced upper ocean stratification with climate change in the CMIP3 models. J. Geophys.
606 Res. 117: C04031, doi:10.1029/2011JC007409
607 Carmack, E., and P. Wassmann. 2006. Food webs and physical-biological coupling on
608 pan-Arctic shelves: unifying concepts and comprehensive perspectives. Progr. Oceanogr. 71:
609 446-477.
610 Carmack, E. C., R. W. Macdonald, R. G. Perkin, F. A. McLaughlin, and R. J. Pearson.
611 1995. Evidence for warming of Atlantic water in the Southern Canadian Basin of the Arctic
612 Ocean: Results from the Larsen-93 Expedition. Geophys. Res. Lett. 22: 1061-1064.
613 Ciais, P., C. Sabine, G. Bala, and others. 2013. Carbon and other biogeochemical cycles.
614 In: Climate Change 2013: The Physical Science Basis. Contribution of Working Group I to
615 the Fifth Assessment Report of the Intergovernmental Panel on Climate Change. T. F.
616 Stocker, D. Qin, G. -K. Plattner, M. Tignor, S. K. Allen, J. Boschung, A. Nauels, Y. Xia, V.
617 Bex, and P.M. Midgle [eds], Cambridge University Press.
618 Coffin, R. B., J. P. Smith, R. E. Plummer, B. Yoza, R. K. Larsen, L. C. Mulholland, and
619 M. T. Montgomery. 2013. Spatial variation in shallow sediment methane sources and cycling
620 on the Alaskan Beaufort Sea shelf/ slope. Mar. Pet. Geol. 45: 186-197.

621 Cordes, E. E., M. A. Arthur, K. Shea, R. S. Arvidson, and C. R. Fisher. 2005. Modeling
622 the mutualistic interactions between tubeworms and microbial consortia. Plos Bio. 3: 497-
623 506.
624 Darcy, H. 1856. Les Fontaines Publiques De La Ville De Dijon. Libraire des Corps
625 Imperiaux des Ponts et Chaussees et des Mines, Paris.
626 de Angelis, M. A., M. D. Lilley, and J. A. Baross. 1993. Methane oxidation in deep-sea
627 hydrothermal plumes of the endeavour segment of the Juan de Fuca Ridge. Deep-Sea Res.
628 Part I 40: 1169-1186.
629 de Beer, D., E. Sauter, H. Niemann, N. Kaul, J. P. Foucher, U. Witte, M. Schluter, and A.
630 Boetius. 2006. In situ fluxes and zonation of microbial activity in surface sediments of the
631 Håkon Mosby Mud Volcano. Limnol. Oceanogr. 51: 1315-1331.
632 DeConto, R. M., S. Galeotti, M. Pagani, D. Tracy, K. Schaefer, T. Zhang, D. Pollard, and
633 D. J. Beerling. 2012. Past extreme warming events linked to massive carbon release from
634 thawing permafrost. Nature 484, 87-91.
635 Deusner, C., V. Meyer, and T. G. Ferdelman. 2010. High-pressure systems for gas-phase
636 free continuous incubation of enriched methane microbial communities performing anaerobic
637 oxidation of methane. Biotechnology and Bioengineering 105: 524-533.
638 Dickens, G. R. 2003. Rethinking the global carbon cycle with a large, dynamic and
639 microbially mediated gas hydrate capacitor. Earth Planet. Sci. Lett. 213: 169-183.
640 Dieser, M., E. L. J. E. Broemsen, K. A. Cameron, and others. 2014. Molecular and
641 biogeochemical evidence for methane cycling beneath the western margin of the Greenland
642 Ice Sheet. ISME Journal 8: 2305-2316.
643 Dlugokencky, E. J., L. Bruhwiler, J. W. C. White, and others. 2009. Observational
644 constraints on recent increases in the atmospheric $CH_4$ burden. Geophys. Res. Lett. 36:
645 L18803, doi:10.1029/2009GL039780

646 Dmitrenko, I. A., S. A. Kirillov, L. B. Tremblay, H. Kassens, O. A. Anismov, S. A.
647 Lavrov, S. O. Razumov, and M. N. Grigoriev. 2011. Recent changes in shelf hydrography in
648 the Siberian Arctic: Potential for subsea permafrost instability. J. Geophys. Res. 116:
649 C10027, doi:10.1029/2011JC007218
650 Elvert, M., and H. Niemann. 2008. Occurrence of unusual steroids and hopanoids derived
651 from aerobic methanotrophs at an active marine mud volcano. Org. Geochem. 39: 167-177.
652 Emanuel, K. A. 1989. Polar lows as Arctic hurricanes. Tellus B 41: 1-17.
653 Ettwig, K. F., M. K. Butler, D. Le Paslier, and others. 2010. Nitrite-driven anaerobic
654 methane oxidation by oxygenic bacteria. Nature 464: 543-548.
655 Felden, J., F. Wenzhoefer, T. Feseker, and A. Boetius. 2010. Transport and consumption
656 of oxygen and methane in different habitats of the Haakon Mosby mud volcano (HMMV).
657 Limon. Oceanogr. 55: 2366-2380.
658 Ferré, B., J. Mienert, and T. Feseker. 2012. Ocean temperature variability for the past 60
659 years on the Norwegian-Svlabard margin influences gas hydrate stability on human time
660 scales. J. Geophys. Res. 117: C10017, doi:10.1029/2012JC008300
661 Fick, A. 1855. Ueber diffusion. Annalen der Physik und Chemie 94: 59-86.
662 Fisher, R. E., Sriskantharajah, S., Lowry, D. and others. 2011. Arctic methane sources:
663 Isotopic evidence for atmospheric inputs. Geophys. Res. let. 38: L21803,
664 doi:10.1029/2011GL049319
665 Francis, J. A., W. Chan, D. J. Leathers, J. R. Miller, and D. E. Veron. 2009. Winter
666 northern hemisphere weather patterns remember summer Arctic sea-ice extent. Geophys.
667 Res. Lett. 36: L07503, doi:10.1029/2009GL037274
668 Gentz, T., E. Damm, J. S. Schneider von Deimling, S. Mau, D. F. McGinnis, and M.
669 Schluter. 2014. A water column study of methane around gas flares located at the West
670 Spitsbergen continental margin. Cont. Shelf. Res. 72: 107-118.

671 Hanson, R. S., and T. E. Hanson. 1996. Methanotrophic bacteria. Microbiological
672 Reviews 60: 439-471.
673 He, X., L. Sun, Z. Xie, W. Huang, N. Long, Z. Li ,and G. Xing. 2013. Sea ice in the Arctic
674 Ocean: Role of shielding and consumption of methane. Atmospheric Environment 67: 8-13.
675 Heeschen, K. U., A. Tréhu, R. W. Collier, E. Suess, and G. Rehder. 2003. Distribution and
676 height of methane bubble plumes on the Cascadia Margin characterized by acoustic imaging.
677 Geophys. Res. Lett. 30: 10.1029/2003GL016974
678 Hinrichs, K. -U., and A. Boetius. 2002. The anaerobic oxidation of methane: New insights
679 in microbial ecology and biogeochemistry, p. 457-477. In G. Wefer, D. Billett, and D.
680 Hebbeln [eds.], Ocean Margin Systems. Springer Verlag.
681 Hinrichs, K. -U., J. M. Hayes, S. P. Sylva, P. G. Brewer, and E. F. DeLong. 1999.
682 Methane-consuming archaebacteria in marine sediments. Nature 398: 802-805.
683 Hubbard, B., and A. Maltman. 2000. Laboratory investigations of the strength, static
684 hydraulic conductivity and dynamic hydraulic conductivity of glacial sediments. Geological
685 Society, London, Special Publications 176: 231-242.
686 Hunter, S. J., D. S. Goldobin, A. M. Haywood, A. Ridgewell, and J. G. Rees. 2013.
687 Sensitivity of the global submarine hydrate inventory to scenarios of future climate change.
688 Earth Planet. Sci. Lett. 367: 105-115.
689 IPCC. 2013. Climate Change 2013: The Physical Science Basis. Contribution of Working
690 Group I to the Fifth Assessment Report of the Intergovernmental Panel on Climate Change.
691 In T. F. Stocker, D. Qin, G. -K. Plattner, M. Tignor, S. K. Allen, J. Boschung, A. Nauels, Y.
692 Xia, V. Bex, and P.M. Midgle [eds], Cambridge University Press.
693 Iversen, N., and T. H. Blackburn. 1981. Seasonal rates of methane oxidation in anoxic
694 marine sediments. Applied and Environmental Microbiology 41:1295-1300.

695 Jacobsen, M. Z. 2004. Climate response of fossil fuel and biofuel soot, accounting for
696 soot's feedback to snow and sea ice albedo and emissivity. J. Geophys. Res. 109: D21201,
697 doi:10.1029/2004JD004945
698 Jakobs, G., P. Holtermann, C. Berndemeyer, G. Rehder, M. Blumenberg, G. Jost, G.
699 Nausch, and O. Schmale. 2014. Seasonal and spatial methane dynamics in the water column
700 of the central Baltic Sea (Gotland Sea). Cont. Shelf Res. 91: 12-25.
701 Jakobsson, M., L. Mayer, B. Coakley, and others. 2012. The International Bathymetric
702 Chart of the Arctic Ocean (IBCAO) Version 3.0. Geophys. Res. Lett. 39: L12609,
703 doi:10.1029/2012GL052219
704 Jones, R. D., and J. A. Amador. 1993. Methane and carbon-monoxide production,
705 oxidation, and turnover times in the Caribbean Sea as influenced by the Orinoco River. J.
706 Geophys. Res. 98: 2353-2359.
707 Kadko, D. C., N. D. Rosenberg, J. E. Lupton, R. W. Collier, and M. D. Lilley. 1990.
708 Chemical reaction rates and entrainment within the Endeavour Ridge hydrothermal plume.
709 Earth Planet. Sci. Lett. 99: 315-335.
710 Kitidis, V., R. C. Upstill-Goddard, and L. G. Anderson. 2010. Methane and nitrous oxide
711 in surface water along the North-West Passage. Arctic Ocean. Mar. Chem. 121: 80-86.
712 Knittel, K., and A. Boetius. 2009. Anaerobic oxidation of methane: progress with an
713 unknown process. Annual Review of Microbiology 63: 311-334.
714 Knittel, K., T. Lösekann, A. Boetius, R. Kort, and R. Amann. 2005. Diversity and
715 distribution of methanotrophic archaea at cold seeps. Applied and Environmental
716 Microbiology 71: 467-479.
717 Kort, E. A., S. C. Wofsy, B. C. Daube, and others. 2012. Atmospheric observations of
718 Arctic Ocean methane emissions up to 82° north. Nature Geosci. 5: 318-321.

719 Kretschmer, K., A. Biastoch, L. Ruepke, and E. Burwicz. 2015. Modeling the fate of
720 methane hydrates under global warming. Global Biogeochem. Cycles 29: 610-625.
721 Kvenvolden, K. A. 1988. Methane hydrate- A major reservoir of carbon in the shallow
722 geosphere. Chem. Geol. 71: 41-51.
723 Kvenvolden, K. A. 1999. Potential effects of gas hydrate on human welfare. Proc. Nat. Ac.
724 Sci. 96: 3420-3426.
725 Lammers, S., E. Suess, Mansurv, M. N., and V. V. Anikiev. 1995. Variations of
726 atmospheric methane supply from the Sea of Okhotsk induced by the seasonal ice cover.
727 Global Biogeochem. Cycles 9: 351-358.
728 Lammers, R. B., A. I. Shiklomanov, C. J. Vorosmarty, B. M. Fekete, and B. J. Peterson.
729 2001. Assessment of contemporary Arctic river runoff based on observational discharge
730 records. J. Geophys. Res. 106: 3321-3334.
731 Leifer, I., and R. K. Patro. 2002. The bubble mechanism for methane transport from the
732 shallow sea bed to the surface: A review and sensitivity study. Cont. Shelf Res. 22: 2409-
733 2428.
734 Leifer, I., and I. R. MacDonald. 2003. Dynamics of the gas flux from shallow gas hydrate
735 deposits: Interaction between oily hydrate bubbles and the oceanic environment. Earth Planet.
736 Sci. Lett. 210: 411-424.
737 Leifer, I., B. P. Luyendyk, J. Boles, and J. F. Clark. 2006. Natural marine seepage
738 blowout: Contribution to atmospheric methane. Global Biogeochemical Cycles 20,
739 doi:10.1029/2005GB002668.
740 Leifer, I., E. Solomon, J. Schneider von Deimling, R. Coffin, G. Rehder, and P. Linke.
741 2015. The fate of bubbles in a large, intense bubble plume for stratified and unstratified
742 water: numerical simulations of 22/4b expedition field data. J. Mar. Pet. Geol. 68: 806-823.

743 Liss, P.S. 1973. Processes of gas exchange across an air-water interface. Deep Sea
744 Research and Oceanographic Abstracts 20: 221-238.
745 Liss, P. S., and L. Merlivat. 1986. Air-sea gas exchange rates: Introduction and synthesis,
746 p. 113-127. In P. Buat-Ménard [ed.], The role of air-sea exchange in geochemical cycling.
747 Springer.
748 Long, Z., and W. Perrie. 2012. Air-sea interactions during an Arctic storm. J. Geophys.
749 Res. 117: D15103, doi:10.1029/2011JD016985
750 Loose, B., W. R. McGillis, D. Perovich, C. J. Zappa, and P. Schlosser. 2014. A parameter
751 model of gas exchange for the seasonal sea ice zone. Ocean. Sci. 10: 17-28.
752 Lösekann, T., K. Knittel, T. Nadalig, B. Fuchs, H. Niemann, A. Boetius, and R. Amann.
753 2007. Diversity and abundance of aerobic and anaerobic methane oxidizers at the Haakon
754 Mosby Mud Volcano, Barents Sea. Applied and Environmental Microbiology 73: 3348-3362.
755 Marìn-Moreno, T. A. Minshull, G. K. Westbrook, B. Sinha, and S. Sarkar. 2013. The
756 response of methane hydrate beneath the seabed offshore Svalbard to ocean warming during
757 the next three centuries. Geophys. Res. Lett. 40, 5159-5163.
758 Martens, C. S., and R. A. Berner. 1974. Methane production in interstitial waters of
759 sulfate-depleted marine sediments. Science 185: 1167-1169.
760 Maslanik, J. A., C. Fowler, J. Stroeve, S. Drobot, H. J. Zwally, D. Yi, and W. J. Emery.
761 2007. A younger, thinner Arctic ice cover: Increased potential for rapid, extensive sea ice
762 loss. Geophys. Res. Lett. 34: L24501, doi:10.1029/2007GL032043
763 Maslowski, W., B. Newton, P. Schlosser, A. Semtner, and D. Martinson. 2000. Modeling
764 recent climate variability in the Arctic Ocean. Geophys. Res. Lett. 27: 3743-3746.
765 Mau, S., J. Blees, E. Helmke, H. Niemann, and E. Damm. 2013. Vertical distribution of
766 methane oxidation and methanotrophic response to elevated methane concentrations in

767 stratified waters of the Arctic fjord Storfjorden (Svalbard, Norway). Biogeosciences 10:
768 6267-6278.
769 McClelland, J. W., S. J. Dery, B. J. Peterson, R. M. Holmes, and E. F. Wood. 2006. A
770 pan-Arctic evaluation of changes in river discharge during the latter half of the 20th century.
771 Geophys. Res. Lett. 33: L06715, doi:10.1029/2006GL025753
772 McGinnis, D. F., J. Greinert, Y. Artemov, S. E. Beaubien, and A. Wuest. 2006. Fate of
773 rising methane bubbles in stratified waters: How much methane reaches the atmosphere? J.
774 Geophys. Res. 111: C09007, doi:10.1029/2005JC003183
775 McGuire, A. D., L. G. Anderson, T. R. Christensen, and others. 2009. Sensitivity of the
776 carbon cycle in the Arctic to climate change. Ecological Monographs 79: 523-555.
777 Murrell, J. C. 2010. The aerobic methane oxidizing bacteria (methanotrophs), p. 1953-
778 1966. In K.N. Timmis [eds.], Handbook of Hydrocarbon and Lipid Microbiology, Springer.
779 Naudts, L., J. Greinert, , Y. Artemov, P. Staelens, J. Poort., P. VanRensbergen, and M.
780 DeBatist. 2006. Geological and morphological setting of 2778 methane seeps in the Dnepr
781 paleo-delta, northwestern Black Sea. Mar. Geol. 227: 177-199.
782 Nauhaus, K., A. Boetius, M. Kruger, and F. Widdel, F. 2002. In vitro demonstration of
783 anaerobic oxidation of methane coupled to sulphate reduction in sediment from a marine gas
784 hydrate area. Environmental Microbiology 4: 296-305.
785 Nauhaus, K., T. Treude, A. Boetius, and M. Kruger. 2005. Environmental regulation of the
786 anaerobic oxidation of methane: a comparison of ANME-I and ANME-II communities,
787 Environmental Microbiology 7, 98-106.
788 Nauhaus, K., M. Albrecht, M. Elvert, A. Boetius, and F. Widdel. 2007. In vitro cell growth
789 of marine archaeal-bacterial consortia during anaerobic oxidation of methane with sulfate.
790 Environmental Microbiology 9: 187-196.

791 Nauw, J., H. de Haas, and G. Rehder. 2015. A review of oceanographic and
792 meteorological controls on the North Sea circulation and hydrodynamics with a view to the
793 fate of North Sea methane from well site 22/4B and other seabed sources. J. Mar. Pet. Geol.
794 68: 861-882.
795 Nielsen, T., T. Laier, A. Kuijpers, T. L. Rasmussen, N. E. Mikkelsen, and N. Norgard-
796 Pedersen. 2014. Fluid flow and methane occurrences in the Disko Bugt area offshore West
797 Greenland: indications for gas hydrates? Geo-Marine Letters 34: 511-523.
798 Niemann, H., and A. Boetius. 2010. Mud Volcanoes, p. 205-214. In K. N. Timmis [eds.],
799 Handbook of Hydrocarbon and Lipid Microbiology. Springer.
800 Niemann, H., M. Elvert, M. Hovland, and others. 2005. Methane emission and
801 consumption at a North Sea gas seep (Tommeliten area). Biogeosciences 2: 335-351.
802 Niemann, H., J. Duarte, C. Hensen, and others. 2006. Microbial methane turnover at mud
803 volcanoes of the Gulf of Cadiz. Geochim. Cosmochim. Acta 70: 5336-5355.
804 Niemann, H., D. Fischer, D. Graffe, and others. 2009. Biogeochemistry of a low-activity
805 cold seep in the Larsen B area, western Weddell Sea, Antarctica. Biogeosciences 6: 2383-
806 2395.
807 Niemann, H., P. Linke, K. Knittel, and others. 2013. Methane-carbon flow into the benthic
808 food web at cold seeps- A case study from the Costa Rica subduction zone. PLoS ONE 8:
809 e74894, doi:10.1371/journal.pone.0074894
810 Nightingale, P.D., G. Malin, C. S. Law, A. J. Watson, P. S. Liss, M. I. Liddicoat, J.
811 Boutin, and R. C. Upstill-Goddard. 2000. In situ evaluation of air-sea gas exchange
812 parameterizations using novel conservative and volatile tracers. Global Biogeochem. Cycles
813 14: 373-387.
814 Nisbet, E. G., and J. Chappellaz. 2009. Shifting gear, quickly. Science 324: 477-478.

Nummelin, A., C. Li, and L. H. Smedsrud. 2015. Response of Arctic Ocean stratification to changing river runoff in a column model. J. Geophys. Res. 120: 2655-2675.

Overduin, P., S. Liebner, C. Knoblauch, F. Günther, S. Wetterich, L. Schirrmeister, H. W. Hubberten, and M. N. Grigoriev. 2015. Methane oxidation following submarine permafrost degradation: Measurements from a central Laptev Sea shelf borehole. J. Geophys. Res. 120: 965-978.

Pape, T., T. Feseker, S. Kasten, D. Fischer, and G. Bohrmann. 2011. Distribution and abundance of gas hydrates in near-surface deposits of the Haakon Mosby Mud Volcano, SW Barents Sea. Geochem. Geophys. Geosyst. 12: Q09009, doi:10.1029/2011GC003575

Parmentier, F. J. W., T. R. Christensen, L. L. Sorensen, S. Rysgaard, A. D. McGuire, P. A. Miller, and D. A. Walker. 2013. The impact of lower sea-ice extent on Arctic greenhouse-gas exchange. Nature Climate Change 3: 195-202.

Paull, C. K., P. G. Brewer, W. Ussler, E. T. Peltzer, G. Rehder, and D. Clague. 2003. An experiment demonstrating that marine slumping is a mechanism to transfer methane from seafloor gas-hydrate deposits into the upper ocean and atmosphere. Geo-Marine Letters 22: 198-203.

Paull, C. K., W. Ussler, S. R. Dallimore, and others. 2007. Origin of pingo-like features on the Beaufort Sea shelf and their possible relationship to decomposing methane gas hydrates. Geophys. Res. Lett. 34: L01603, doi:10.1029/2006GL027977

Pickart, R. S., M. A. Spall, and J. T. Mathis. 2013. Dynamics of upwelling in the Alaskan Beaufort Sea and associated shelf–basin fluxes. Deep Sea Res. Part 1 76: 35-51.

Pohlman, J., C. Ruppel, C. Maue, L. Brothers, J. Kessler, and C. Worley. 2012. Real-time mapping of seawater and atmospheric methane concentrations offshore Alaska's north slope. Sound Waves (USGS Newsletter), May-June 2012.

Polyakov, I. V., L. A. Timokhov, V. A. Alexeev, and others. 2010. Arctic Ocean warming contributes to reduced polar ice cap. J. Phys. Oceanography 40: 2743-2756.

Popova, E. E., A. Yool, Y. Aksenov, A. C. Coward, and T. R. Anderson. 2014. Regional variability of acidification in the Arctic: a sea of contrasts. Biogeosciences, 11: 293-308.

Rachold, V. D., D. Y. Bolshyanov, M. N. Grigoriev, and others. 2007. Nearshore Arctic subsea permafrost in transition. EOS Trans. AGU 88: 149.

Reagan, M. T., and G. J. Moridis. 2009. Large-scale simulation of methane hydrate dissociation along the West Spitsbergen Margin. Geophys. Res. Lett., 36: L23612, doi:10.1029/2009GL041332

Reagan, M. T., G. J. Moridis, S. M. Elliott, and M. Maltrud. 2011. Contribution of oceanic gas hydrate dissociation to the formation of Arctic Ocean methane plumes. J. Geophys. Res. 116: C09014, doi:10.1029/2011JC007189

Reeburgh, W. S. 2007. Oceanic methane biogeochemistry. Chemical Reviews 107: 486-513.

Rehder, G., R. S. Keir, E. Suess, and M. Rhein. 1999. Methane in the Northern Atlantic controlled by microbial oxidation and atmospheric history. Geophys. Res. Lett. 26: 587-590.

Rehder, G., R. W. Collier, K. Heeschen, P. M. Kosro, J. Barth, and E. Suess. 2002. Enhanced marine $CH_4$ emissions to the atmosphere off Oregon caused by coastal upwelling. Global Biogeochem. Cycles 3, doi:10.1029/2000GB001391

Rehder, G., I. Leifer, P. G. Brewer, G. Friederich, and E. T. Peltzer. 2009. Controls on methane bubble dissolution inside and outside the hydrate stability field from open ocean field experiments and numerical modelling. Mar. Chem. 114: 19-30.

Rother, M. 2010. Methanogenesis, p. 483-499. In K. N. Timmis [ed.], Handbook of hydrocarbon and lipid microbiology, Vol 1. Springer.

Rudd, J. W. M., A. Furutani, R. J. Flett, and R. D. Hamilton. 1976. Factors controlling methane oxidation in shield lakes: The role of nitrogen fixation and oxygen concentration. Limnol. Oceanogr. 21: 357-364.

Rudd, J. W. M., and R. D. Hamilton. 1978. Methane cycling in a eutrophic shield lake and its effects on whole lake metabolism. Limnol. Oceanogr. 23: 337-348.

Rudels, B., A. -M. Larsson, and P. -I. Sehlstedt. 1991. Stratification and water mass formation in the Arctic Ocean: Some implications for the nutrient distribution. Polar Research 10: 19-32.

Sarkar, S., C. Berndt, T. A. Minshull, G. K. Westbrook, D. Klaeschen, D. G. Masson, A. Chabert, and K. E. Thatcher. 2012. Seismic evidence for shallow gas-escape features associated with a retreating gas hydrate zone offshore west Svalbard. J. Geophys. Res. 117: B09102, doi:10.1029/2011JB009126

Schmale, O., I. Leifer, J. Schneider von Deimling, C. Stolle, S. Krause, K. Kießlich, A. Frahm, and T. Treude. 2015. Bubble Transport Mechanism: Indications for a gas bubble-mediated inoculation of benthic methanotrophs into the water column. Contin. Shelf Res. 103: 70-78.

Schneider, B., W. Gulzow, B. Sadkowiak, and G. Rehder. 2014. Detecting sinks and sources of $CO_2$ and $CH_4$ by ferrybox-based measurements in the Baltic Sea: Three case studies. J. Mar. Syst. 140: 13-25.

Schneider von Deimling, J., G. Rehder, J. Greinert, D. F. McGinnis, A. Boetius, and P. Linke. 2011. Quantification of seep-related methane gas emissions at Tommeliten, North Sea. Cont. Shelf Res. 31: 867-878.

Schneider von Deimling, J., P. Linke, M. Schmidt, and G. Rehder. 2015. Ongoing methane discharge at well site 22/4b (North Sea) and discovery of a spiral vortex bubble plume motion. J. Mar. Pet. Geol. 68: 718-730.

888 Schuur, E. A. G., A. D. McGuire, C. Schädel, and others. 2015. Climate change and the
889 permafrost carbon feedback. Nature 520: 171-179.
890 Scranton, M. I., and P. G. Brewer. 1978. Consumption of dissolved methane in the deep
891 ocean. Limnol. Oceanogr. 23: 1207-1213.
892 Selim, M. S., and E. D. Sloan. 1989. Heat and mass transfer during the dissociation of
893 hydrates in porous media. AIChE Journal 35: 1049-1052.
894 Semiletov, I. P., N. I. Savelieva, G. E. Weller, I. I. Pipko, S. P. Pugach, A. Y. Gukov, and
895 L. N. Vasilevskaya. 2000. The dispersion of Siberian river flows into coastal waters:
896 Meteorological, hydrological and hydrochemical aspects, p. 323-366. In E. L. Lewis, E. P.
897 Jones, P. Lemke, T. D. Prowse and P. Wadhams [eds.], Freshwater budget of the Arctic
898 Ocean. Springer.
899 Serreze, J. M. 2011. Rethinking the sea-ice tipping point. Nature 471: 47-48.
900 Shakhova, N., I. Semiletov, A. Salyu, V. Yusupov, D. Kosmach, and Ö. Gustafsson. 2010.
901 Extensive methane venting to the atmosphere from sediments of the East Siberian Arctic
902 Shelf. Science 327: 1246-1250.
903 Shakhova, N., I. Semiletov, I. Leifer, and others. 2014. Ebullition and storm-induced
904 methane release from the East Siberian Arctic Shelf. Nature Geosci. 7: 64-70.
905 Sivan, O., M. Adler, A. Pearson, F. Gelman, I. Bar-Or, S. G. John, and W. Eckert. 2011.
906 Geochemical evidence for iron-mediated anaerobic oxidation of methane. Limnol. Oceanogr.
907 56: 1536-1544.
908 Sloan Jr., E. D., and C. Koh. 2007. Clathrate hydrates of natural gases, 3rd ed. CRC Press.
909 Smith, J.A. 1998. Evolution of Langmuir circulation during a storm. J. Geophys. Res. 103:
910 12649-12668.

911 Smith, A.J., J. Mienert, S. Bünz, and J. Greinert. 2014. Thermogenic methane injection via
912 bubble transport into the upper Arctic Ocean from the hydrate-charged Vestnesa Ridge,
913 Svalbard. Geochem. Geophys. Geosyst. a5: 1945-1959.
914 Steinle, L., C. A. Graves, T. Treude, and others. 2015. Water column methanotrophy
915 controlled by a rapid oceanographic switch. Nature Geosci. 8: 378-382.
916 Stroeve, J., M. Serreze, S. Drobot, S. Gearheard, M. Holland, J. Maslanik, W. Meier, and
917 T. Scambos. 2008. Arctic sea ice extent plummets in 2007. Eos Trans. AGU 89: 13.
918 Stroeve, J. C., J. Maslanik, M. C. Serreze, I. Rigor, W. Meier, and C. Fowler. 2011. Sea
919 ice response to an extreme negative phase of the Arctic Oscillation during winter 2009/2010.
920 Geophys. Res. Lett. 38: L02502, doi:10.1029/2010GL045662
921 Thatcher, K. E., G. K. Westbrook, S. Sarkar, and T. A. Minshull. 2013. Methane release
922 from warming-induced hydrate dissociation in the West Svalbard continental margin:
923 Timing, rates, and geological controls. J. Geophys. Res. 118: 22-38.
924 Thomson, J., and W. E. Rogers. 2014. Swell and sea in the emerging Arctic Ocean.
925 Geophys. Res. Lett. 41: 3136-3140.
926 Tomonaga, Y., M. S. Brennwald, and R. Kipfer. 2015. Attenuation of diffusive noble-gas
927 transport in laminated sediments of the Stockholm Archipelago. Limnol. Oceanogr. 60: 497-
928 511.
929 Treude, T., A. Boetius, K. Knittel, K. Wallmann, and B. B. Jørgensen. 2003. Anaerobic
930 oxidation of methane above gas hydrates at Hydrate Ridge, NE Pacific Ocean. Mar. Ecol.
931 Prog. Ser. 264: 1-14.
932 Treude, T., M. Kruger, A. Boetius, and B. B. Jørgensen. 2005. Environmental control on
933 anaerobic oxidation of methane in the gassy sediments of Eckernforde Bay (German Baltic).
934 Limnol. Oceanogr. 50: 1771-1786.

Treude, T., S. Krause, J. Maltby, A. W. Dale, R. Coffin, and L. J. Hamdan. 2014. Sulfate reduction and methane oxidation below the sulfate-methane transition zone in Alaskan Beaufort Sea continental margin sediments: implications for sulphur cycling. Geochim. Cosmochim. Acta 144: 217-237.

Valentine, D. L., C. M. Reddy, C. Farwell, and others. 2010. Asphalt volcanoes as a potential source of methane to late Pleistocene coastal waters. Nature Geosci. 3: 345-348.

Vanneste, M., C. Berndt, J. S. Laberg, and J. Mienert. 2007. On the origin of large shelf embayments on glaciated margins- effects of lateral ice flux variations and glacio-dynamics west of Svalbard. Quat. Sci. Rev. 26: 2406-2419.

Wåhlström, I., and H. E. M. Meier. 2014. A model sensitivity study for the sea-air exchange of methane in the Laptev Sea, Arctic Ocean. Tellus B 66: 24174, doi:10.3402/tellusb.v66.24174

Walczowski, W., and J. Piechura. 2006. New evidence of warming propagating toward the Arctic Ocean. Geophys. Res. Lett. 33: L12601, doi:10.1029/2006GL025872

Wang, M., and J. E. Overland. 2009. A sea ice free summer Arctic within 30 years? Geophys. Res. Lett. 36: L07502, doi:10.1029/2009GL037820

Wanninkhof, R. 1992. Relationship between wind speed and gas exchange over the ocean. J. Geophys. Res. 97: 7373-7382.

Wanninkhof, R., and W. R. McGillis. 1999. A cubic relationship between air-sea $CO_2$ exchange and wind speed. Geophys. Res. Lett. 26: 1889-1892.

Wanninkhof, R., W. E. Asher, D. T. Ho, C. S. Sweeney, and W. R. McGillis. 2009. Advances in quantifying air-sea gas exchange and environmental forcing. Ann. Rev. Mar. Sci. 1: 213-244

Ward, B. B., K. A. Kilpatrick, P. C. Novelli, P. C., and M. I. Scranton. 1987. Methane oxidation and methane fluxes in the ocean surface-layer and deep anoxic waters. Nature 327: 226-229.

Ward, B. B., K. A. Kilpatrick, A. E. Wopat, E. C. Minnich, and M. E. Lidstrom. 1989. Methane oxidation in Saanich Inlet during summer stratification. Cont. Shelf. Res. 9: 65-75.

Westbrook, G. K., K. E. Thatcher, E. J. Rohling, and others. 2009. Escape of methane gas from the seabed along the West Spitsbergen continental margin.Geophys. Res. Lett. 36: L15608, doi:10.1029/2009GL039191

Wilfert, P., S. Krause, V. Liebetrau, J. Schönfeld, M. Haeckel, P. Linke, and T. Treude. 2015. Response of anaerobic methanotrophs and benthic foraminifera on 20 years of methane emission from a gas blowout in the North Sea. J. Mar. Pet. Geol. doi:10.1016/j.marpetgeo.2015.07.012

Woodgate, R. A., K. Aagaard, and T. J. Weingartner. 2006. Interannual changes in the Bering Strait fluxes of volume, heat and freshwater between 1991 and 2004. Geophys. Res. Lett. 33: L15609, doi:10.1029/2006GL026931

Yang, D., D. L. Kane, L. D. Hinzman, X. Zhang, T. Zhang, and H. Ye. 2002. Siberian Lena River hydrologic regime and recent change. J. Geophys. Res. 107: 4694.

Zahn, M., and H. von Storch. 2010. Decreased frequency of North Atlantic polar lows associated with future climate warming. Nature 467: 309-312.

Zehnder, A. J. B., and Brock, T. D. 1980. Anaerobic methane oxidation: Occurrence and ecology. Applied and Environmental Microbiology 39: 194-204.

Zhang, J., R. Lindsay, A. Schweiger, and M. Steele. 2013. The impact of an intense summer cyclone on 2012 Arctic sea ice retreat. Geophys. Res. Lett. 40: 720–726.

**Acknowledgments**

All authors gratefully acknowledge support from the European Cooperation in Science and Technology (COST) Action ES0902. Additional support was provided by: The UK Natural Environment Research Council (NE/D005728/2) and Department of Energy, Environment and Climate Change (RHJ); European Space Agency (ESA) Support to Science Element (STSE) OceanFlux Greenhouse Gases Evolution project (4000112091/14/I-LG) and National Science Center, Poland (NCN) Growing of Arctic Ecosystem (GAME) project (DEC-2012/04/A/NZ8/00661) (JP); the European Union Seventh Framework Programme (FP7/2007-2013) under the MIDAS project, grant agreement # 603418 (MH & LV); the Research Council of Norway through its Centres of Excellence funding scheme grant # 223259 (JG, HN).

**Figure Legends**

**Figure 1:** Bathymetric map of the Arctic Ocean, showing shallow coastal seas. Adapted from Jakobsson et al. (2012).

**Figure 2:** September sea-ice minimum in the Arctic 1979-2014. Data courtesy of the Alfred Wegner Institut and Universität Bremen (http://meerisportal.de).

**Figure 3:** Schematic diagram of the occurrence and distribution of hydrate in the Arctic Ocean. The intersection of the water column and geothermal gradient with the hydrate stability curve controls the depth interval in which hydrate can form if pore water is saturated with methane.

**Figure 4:** Hydroacoustic image of gas bubble plumes rising from the seafloor in ~1880 m water depth within the gas hydrate stability zone offshore western Svalbard. Note the depressions, or pockmarks, in the seafloor (shown in dark brown) immediately below the plumes (see Smith et al., 2014). Note that the ship turned through 180° at ~13:10; all flares are tilted to the northeast as that is the direction of the prevailing current.

**Figure 5:** Methane consumption by (i) anaerobic oxidation of methane, and (ii) aerobic methane oxidation. Note that methane gas can bypass microbially mediated oxidation reactions because microbes can only access dissolved methane.

**Figure 6:** Proportion of methane remaining in a gas bubble relative to the initial (i) methane concentration in a bubble released at the seabed, for bubbles with initial radii of 3mm and 5mm, released at 90 m and 400 m water depth. The green dashed line shows the upper limit of the gas hydrate stability zone (GHSZ) on the Arctic continental slope.

**Figure 7:** Compilation of methane turnover time versus ambient methane concentration, for various marine environments. Note logarithmical scale. Data from Ward et al. (1987), Ward et al. (1989), Kadko et al. (1990), de Angelis et al. (1993), Jones and Amador (1993), and Steinle et al. (2015) were determined using either $^{14}C$ or $^{3}H$ labelling techniques, while the

studies by Scranton and Brewer (1978) and Rehder et al. (1999) were determined using tracer/tracer relations. Data from Kadko et al. (1990) and de Angelis et al. (1993) are for hydrothermal systems. Figure modified from Nauw et al. (2015).

**Table 1:** Estimates of the methane inventory of Arctic marine sediments. The methane inventory for the atmosphere, and the inventory of organic carbon in northern high latitude terrestrial permafrost (that has the potential for release as $CH_4$ and $CO_2$), are also shown for comparison.

| Reservoir | Inventory (Gt $CH_4$) | Reference |
|---|---|---|
| *Marine sediments* | | |
| Methane hydrate | 30-9000* | Kvenvolden (1988); McGuire et al. (2009); Biastoch et al., 2011; Hunter et al. (2013); Kretschmer et al. (2015) |
| Submerged permafrost | 2-1400† | McGuire et al. (2009); Shakhova et al. (2010) |
| *Terrestrial* | | |
| Permafrost carbon | 1330-1580†† | Schuur et al. (2015) |
| *Atmospheric burden* | | |
| 2011 | 4.95±0.01 | Ciais et al. (2013) |

*Estimates of the quantity of methane stored in gas hydrate are strongly dependent on hydrate saturation. The consensus converges on values of a few hundred Gt.

†These values are highly uncertain. McGuire et al. (2009) give a figure of 2-65 Gt for the entire Arctic; Shakhova et al. (2010) report that ~1400 Gt alone is stored on the East Siberian Arctic shelf; ~540 Gt as hydrate and ~360 Gt as free gas trapped beneath the permafrost.

††Gt C.

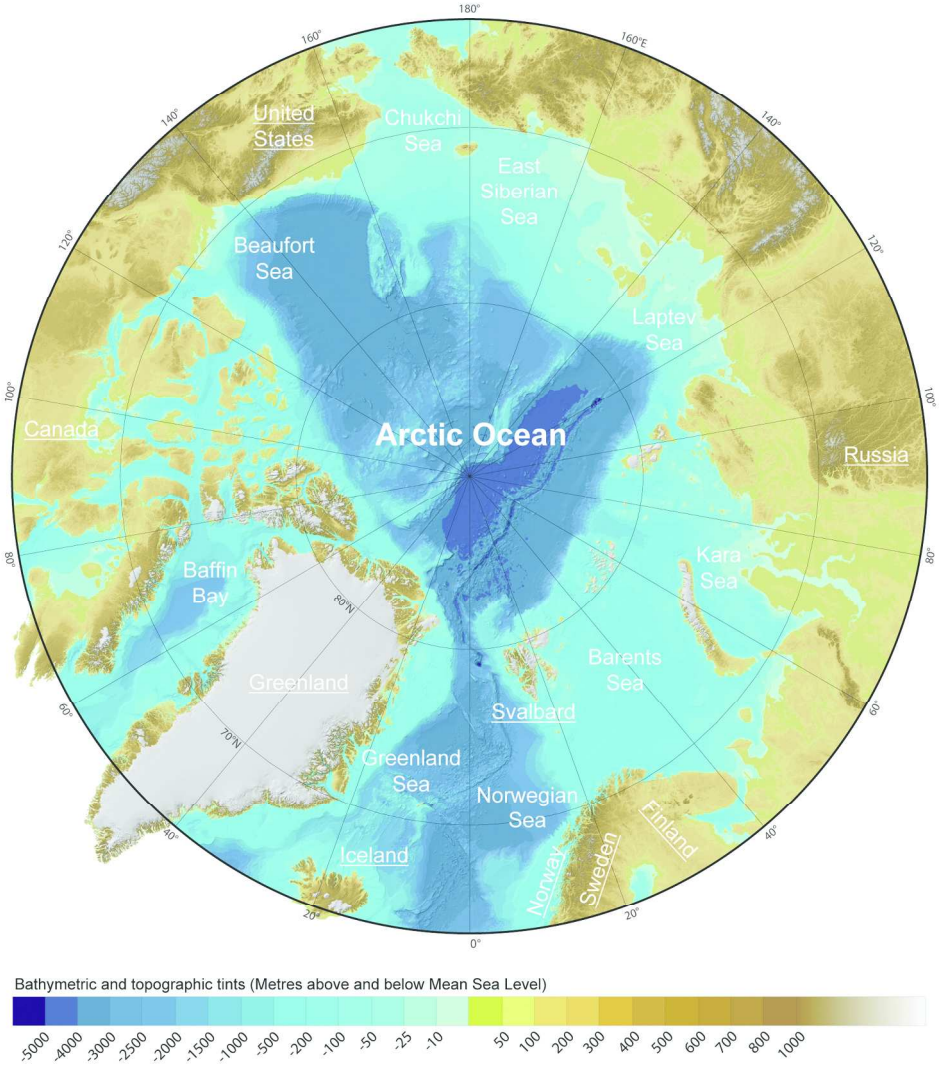


Figure 1. Bathymetric map of the Arctic Ocean, showing shallow coastal seas. Adapted from Jakobsson et al. (2012).
181x201mm (300 x 300 DPI)

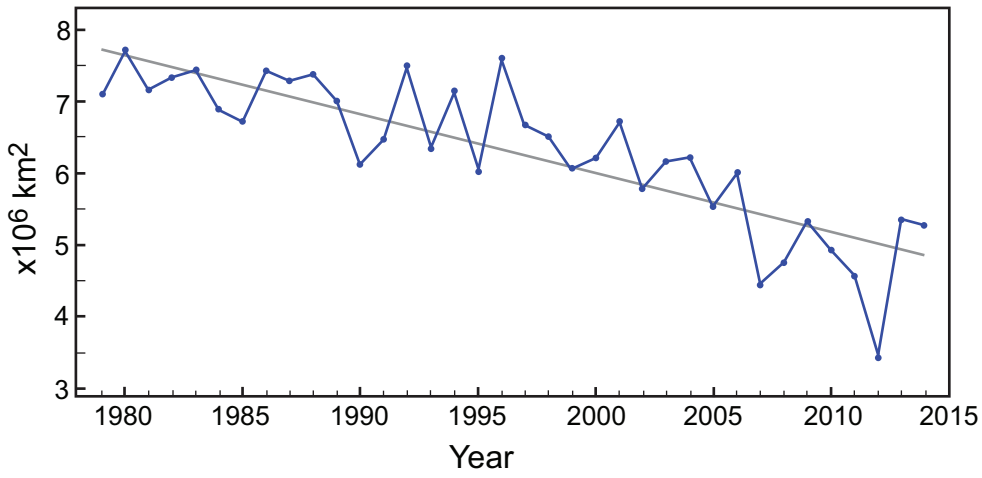
8
7
6
5
4
3
x10^6 km^2
1980
1985
1990
1995
2000
2005
2010
2015
Year

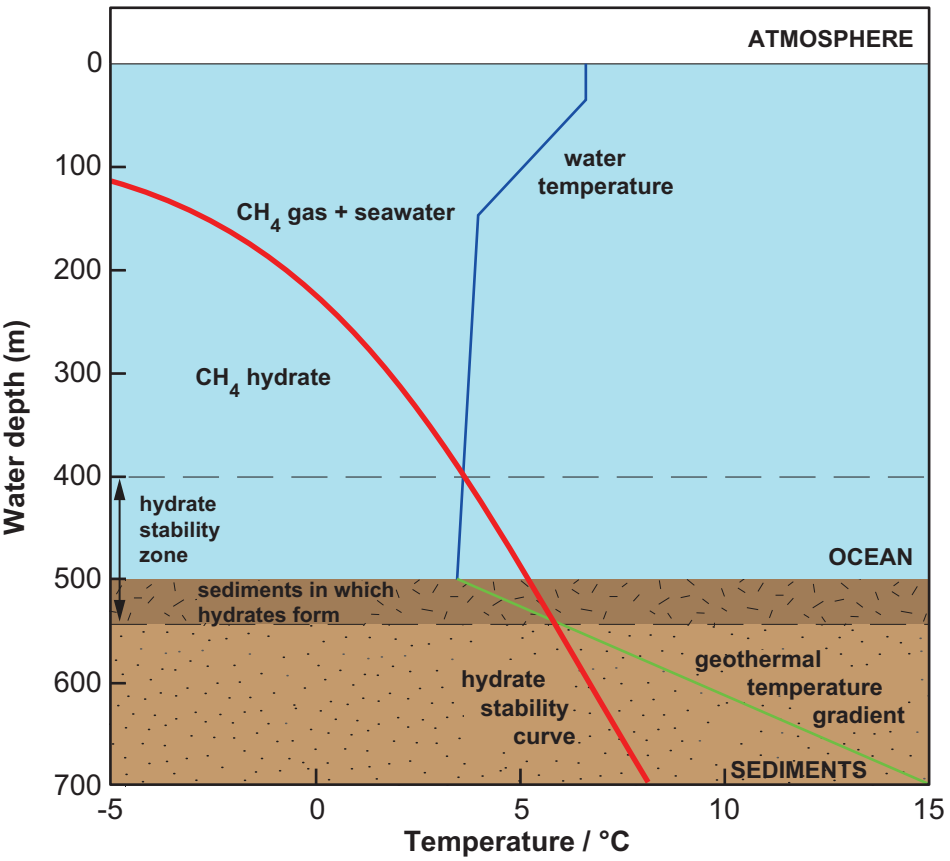
ATMOSPHERE
0
100
200
300
400
500
600
700
Water depth (m)
water temperature
CH4 gas + seawater
CH4 hydrate
hydrate stability zone
OCEAN
sediments in which hydrates form
geothermal temperature gradient
hydrate stability curve
SEDIMENTS
-5
0
5
10
15
Temperature / °C

Fig. 3

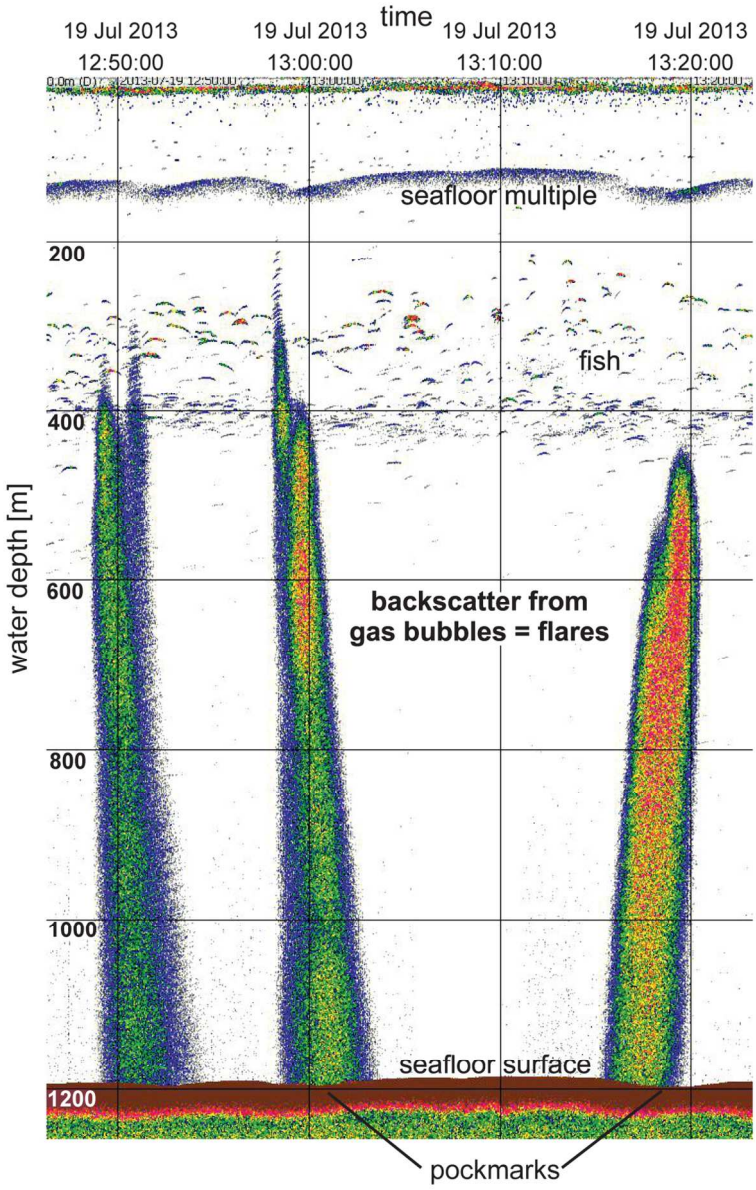


Figure 4: Hydroacoustic image of gas bubble plumes rising from the seafloor in ~1880 m water depth within the gas hydrate stability zone offshore western Svalbard. Note the depressions, or pockmarks, in the seafloor (shown in dark brown) immediately below the plumes (see Smith et al., 2014). Note that the ship turned through 180° at ~13:10; all flares are tilted to the northeast as that is the direction of the prevailing current.
100x152mm (300 x 300 DPI)

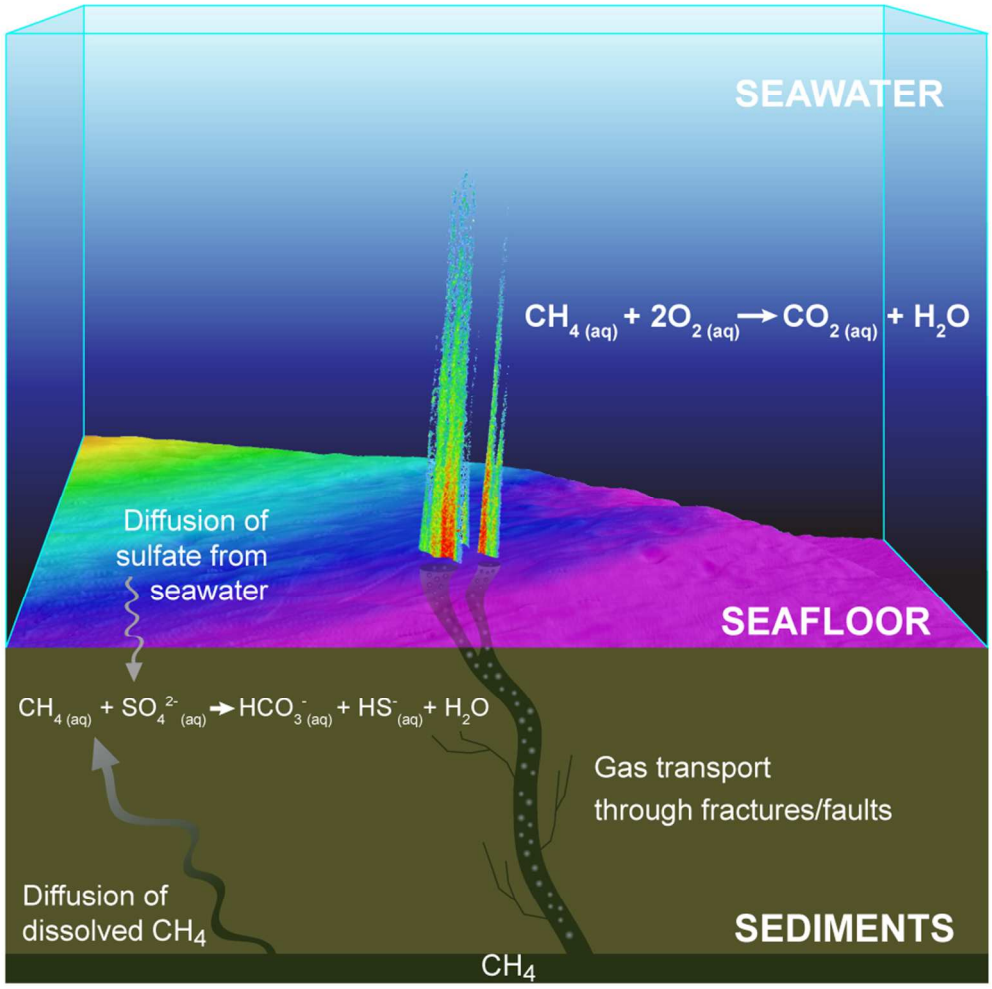


Figure 5: Methane consumption by (i) anaerobic oxidation of methane, and (ii) aerobic methane oxidation. Note that methane gas can bypass microbially mediated oxidation reactions because microbes can only access dissolved methane.
85x86mm (300 x 300 DPI)

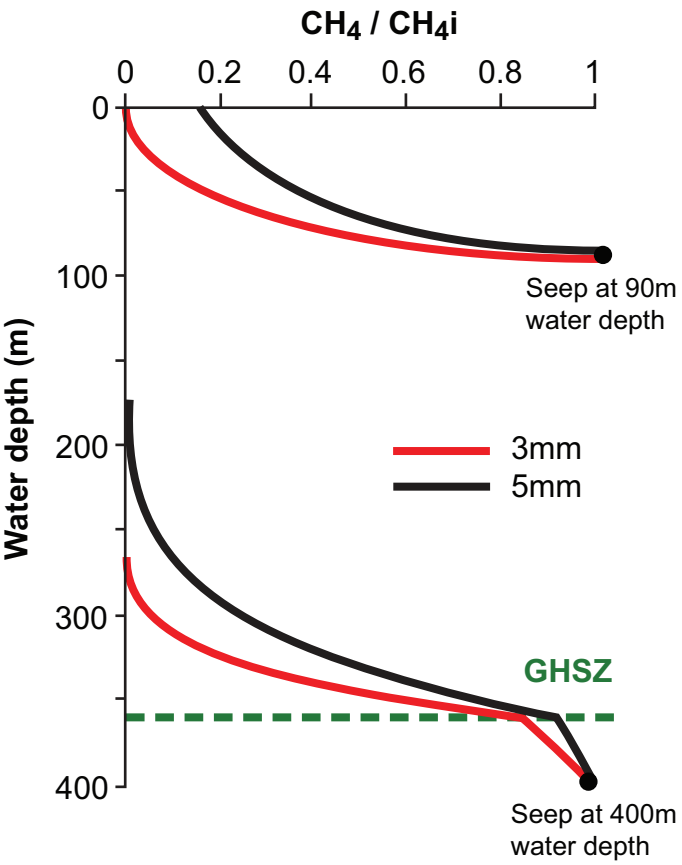
CH4 / CH4i
0
0.2
0.4
0.6
0.8
1
0
100
200
300
400
Water depth (m)
Seep at 90m
water depth
3mm
5mm
GHSZ
Seep at 400m
water depth

Fig. 6

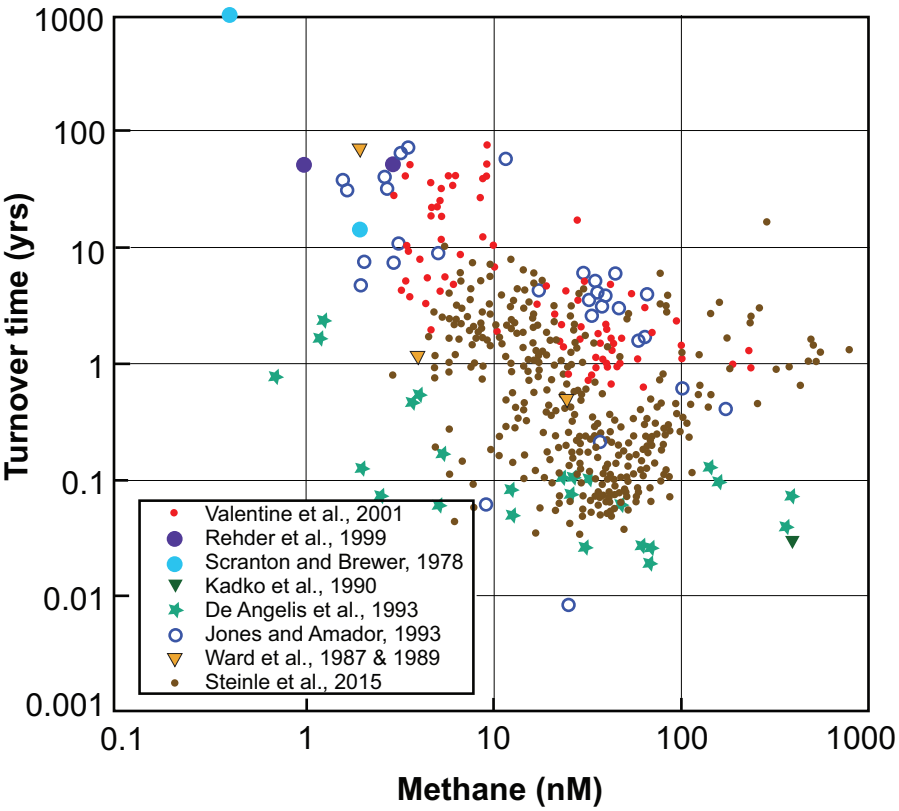
1000
100
10
1
0.1
0.01
0.001
Turnover time (yrs)
0.1
1
10
100
1000
Methane (nM)
Valentine et al., 2001
Rehder et al., 1999
Scranton and Brewer, 1978
Kadko et al., 1990
De Angelis et al., 1993
Jones and Amador, 1993
Ward et al., 1987 & 1989
Steinle et al., 2015

Fig. 7